pseudogap energy scale (*23*, *29*) coexist with these low-energy dispersive modulations at all temperatures studied. Third, analysis of the data using the octet model provides a new perspective on the superconducting energy gap at lowest dopings, indicating that an arc of gapless excitations exists in the strongly underdoped superconducting phase (*22*, *23*, *30*) and that it expands linearly in temperature. Such an arc might exist either due to effects of scattering (*31*, *32*) or due to phase fluctuations (*6*) that are generated by a purely quantum mechanical processes (*7–12*, *34*), or both. Fourth, as the alterations in interference intensities (Fig. 4) that are detected with increasing temperature mimic those generated by introduction of static vortices at low temperatures (*30*), it may be that they occur here for similar reasons but now in a nonstatic vortex fluid (*13–17*). Finally, our observations reveal that the electronic structure of the strongly underdoped pseudogap regime contains not two, but three fundamental components: (i) the Fermi arc (*24*), (ii) the gap $\pm|\Delta(\vec{k})|$ of a phase-disordered superconductor to coherent *k*-space excitations, and (iii) the nondispersive and locally symmetry-breaking excitations at the pseudogap energy scale (*23*, *29*).

References and Notes

1. M. Randeria, N. Trivedi, A. Moreo, R. T. Scalettar, *Phys. Rev. Lett.* **69**, 2001 (1992).
2. V. J. Emery, S. A. Kivelson, *Nature* **374**, 434 (1995).
3. M. Franz, A. J. Millis, *Phys. Rev. B* **58**, 14572 (1998).
4. E. W. Carlson, S. A. Kivelson, V. J. Emery, E. Manousakis, *Phys. Rev. Lett.* **83**, 612 (1999).
5. H.-J. Kwon, A. T. Dorsey, P. J. Hirschfeld, *Phys. Rev. Lett.* **86**, 3875 (2001).
6. E. Berg, E. Altman, *Phys. Rev. Lett.* **99**, 247001 (2007).
7. M. Franz, Z. Tešanović, *Phys. Rev. Lett.* **87**, 257003 (2001).
8. I. F. Herbut, *Phys. Rev. Lett.* **88**, 047006 (2002).
9. M. Hermele, T. Senthil, M. P. A. Fisher, *Phys. Rev. B* **72**, 104404 (2005).
10. E.-A. Kim *et al.*, *Phys. Rev. B* **77**, 184514 (2008).
11. A. Pelissetto, S. Sachdev, E. Vicari, *Phys. Rev. Lett.* **101**, 027005 (2008).
12. M. Grilli, G. Seibold, A. D. Ciolo, J. Lorenzana, *Phys. Rev. B* **79**, 125111 (2009).
13. J. Corson, R. Mallozzi, J. Orenstein, J. N. Eckstein, I. Bozovic, *Nature* **398**, 221 (1999).
14. Z. A. Xu, N. P. Ong, Y. Wang, T. Kakeshita, S. Uchida, *Nature* **406**, 486 (2000).
15. Y. Wang, L. Li, N. P. Ong, *Phys. Rev. B* **73**, 024510 (2006).
16. Y. Wang *et al.*, *Phys. Rev. Lett.* **95**, 247002 (2005).
17. L. Li *et al.*, *Europhys. Lett.* **72**, 451 (2005).
18. N. Bergeal *et al.*, *Nat. Phys.* **4**, 608 (2008).
19. O. Cyr-Choinière *et al.*, *Nature* **458**, 743 (2009).
20. J. E. Hoffman *et al.*, *Science* **297**, 1148 (2002).
21. K. McElroy *et al.*, *Nature* **422**, 592 (2003).
22. T. Hanaguri *et al.*, *Nat. Phys.* **3**, 865 (2007).
23. Y. Kohsaka *et al.*, *Nature* **454**, 1072 (2008).
24. M. R. Norman *et al.*, *Nature* **392**, 157 (1998).
25. T. Pereg-Barnea, M. Franz, *Phys. Rev. B* **68**, 180506 (2003).
26. S. Misra, M. Vershinin, P. Phillips, A. Yazdani, *Phys. Rev. B* **70**, 220503 (2004).
27. D. Wulin, Y. He, C.-C. Chien, D. K. Morr, K. Levin, *Condens. Matt.*, preprint available at http://arxiv.org/abs/0904.3114v1 (2009).
28. M. Vershinin *et al.*, *Science* **303**, 1995 (2004).
29. Y. Kohsaka *et al.*, *Science* **315**, 1380 (2007).
30. T. Hanaguri *et al.*, *Science* **323**, 923 (2009).
31. S. Haas, A. V. Balatsky, M. Sigrist, T. M. Rice, *Phys. Rev. B* **56**, 5108 (1997).
32. A. V. Chubukov, M. R. Norman, A. J. Millis, E. Abrahams, *Phys. Rev. B* **76**, 180501(R) (2007).
33. A. Kanigel *et al.*, *Nat. Phys.* **2**, 447 (2006).
34. I. Hetel, T. R. Lemberger, M. Randeria, *Nat. Phys.* **3**, 700 (2007).

35. We acknowledge and thank J. C. Campuzano, T. Hanaguri, M. Franz, P. J. Hirschfeld, D.-H. Lee, S. Kivelson, Y. Kohsaka, E.–A. Kim, M. Lawler, J. Lee, K. Levin, D. Morr, M. Norman, N. P. Ong, J. Orenstein, M. Randeria, S. Sachdev, H. Takagi, and A. Tsvelik for helpful discussions and communications. These studies are supported by Brookhaven National Laboratory, the U.S. Department of Energy, the U.S. Office of Naval Research, by Grant-in-Aid for Scientific Research from the Ministry of Science and Education (Japan), and by the Global Centers of Excellence Program for Japan Society for the Promotion of Science. A.S. acknowledges support from the U.S. Army Research Office.

Supporting Online Material
www.sciencemag.org/cgi/content/full/325/5944/1099/DC1
Materials and Methods
SOM Text
Figs. S1 to S8
References
Movies S1 to S6

15 May 2009; accepted 17 July 2009
10.1126/science.1176369

Strong Coupling Between Single-Electron Tunneling and Nanomechanical Motion

G. A. Steele,* A. K. Hüttel,† B. Witkamp, M. Poot, H. B. Meerwaldt, L. P. Kouwenhoven, H. S. J. van der Zant

Nanoscale resonators that oscillate at high frequencies are useful in many measurement applications. We studied a high-quality mechanical resonator made from a suspended carbon nanotube driven into motion by applying a periodic radio frequency potential using a nearby antenna. Single-electron charge fluctuations created periodic modulations of the mechanical resonance frequency. A quality factor exceeding 10^5 allows the detection of a shift in resonance frequency caused by the addition of a single-electron charge on the nanotube. Additional evidence for the strong coupling of mechanical motion and electron tunneling is provided by an energy transfer to the electrons causing mechanical damping and unusual nonlinear behavior. We also discovered that a direct current through the nanotube spontaneously drives the mechanical resonator, exerting a force that is coherent with the high-frequency resonant mechanical motion.

Nanomechanical systems (*1*, *2*) have promising applications, such as ultrasensitive mass detection (*3–5*). The combination of a high resonance frequency and a small mass also makes nanomechanical resonators attractive for a fundamental study of mechanical motion in the quantum limit (*6–9*). For a successful observation of quantum motion of a macroscopic object, a high-frequency nanoscale resonator must have low dissipation (which implies a high quality factor *Q*) and a sensitive detector with minimum back-action (i.e., quantum limited) (*10*, *11*). In our experiment, we demonstrate a dramatic back-action that strongly couples a quantum-dot detector to the resonator dynamics of a carbon nanotube, and which, in the limit of strong feedback, spontaneously excites large-amplitude resonant mechanical motion.

Nanomechanical resonators have been created by etching down larger structures. In small devices, however, surfaces effects impose an upper limit on *Q* (*2*). Alternatively, suspended carbon nanotubes can be used to avoid surface damage from the (etching) fabrication process. We recently developed a mechanical resonator based on an ultraclean carbon nanotube with high resonance frequencies of several hundred megahertz and a *Q* exceeding 10^5 (*12*). Here, we use this resonator to explore a strong coupling regime between single-electron tunneling and nanomechanical motion. We followed the pioneering approaches in which aluminum single-electron transistors were used as position detectors (*6–8*) and atomic force microscopy cantilevers as resonators (*13–15*); however, our experiment is in the limit of much stronger electro-mechanical coupling, achieved by embedding a quantum-dot detector in the nanomechanical resonator itself.

Our device consists of a nanotube suspended across a trench that makes electrical contact to two metal electrodes (Fig. 1). Electrons are confined in the nanotube by Schottky barriers at the Pt metal contacts, forming a quantum dot in the suspended segment. The nanotube growth is the last step in the fabrication process, yielding ultraclean devices (*16*), as demonstrated by the fourfold shell filling of the Coulomb peaks (Fig. 1C). We performed all measurements at 20 mK with an electron temperature of ~80 mK.

Kavli Institute of NanoScience, Delft University of Technology, Post Office Box 5046, 2600 GA, Delft, Netherlands.

*To whom correspondence should be addressed. E-mail: g.a.steele@tudelft.nl

†Present address: Institute for Experimental and Applied Physics, University of Regensburg, 93040 Regensburg, Germany.

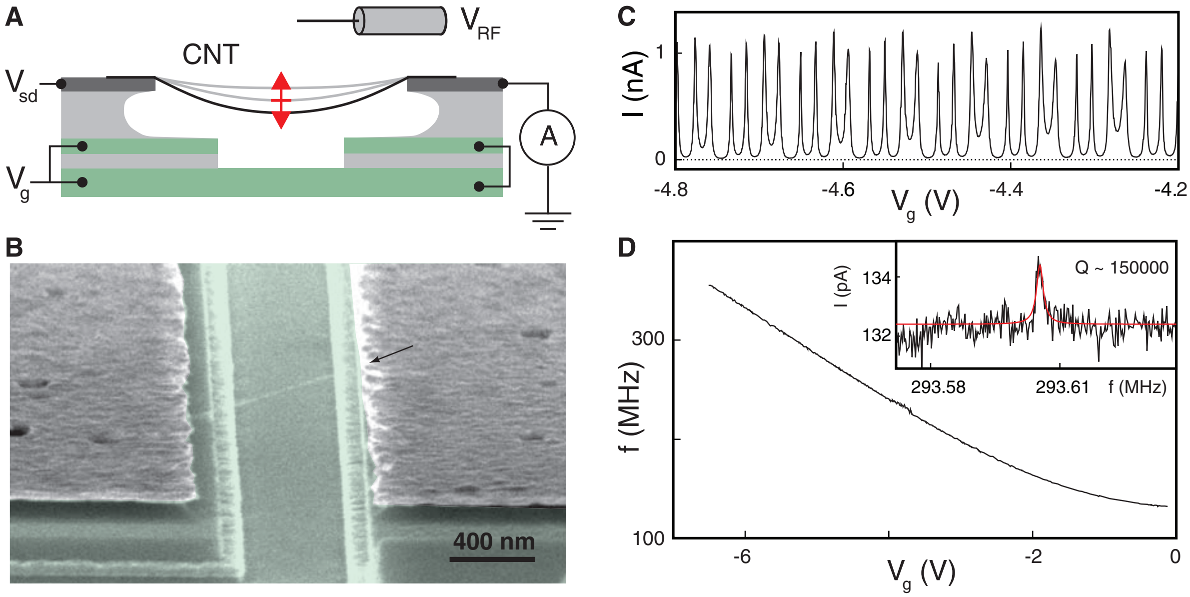

Fig. 1. A high-Q nanotube mechanical resonator with an embedded quantum dot. (**A**) Device layout. A suspended carbon nanotube is excited into mechanical motion by applying an ac voltage to a nearby antenna. A dc current through the nanotube detects the motion. V_{RF}, radio frequency voltage; CNT, carbon nanotube. (**B**) Scanning electron microscopy image of a typical device. The arrow indicates the position of a nanotube. (**C**) A quantum dot, formed between Schottky barriers at the metal contacts, displays fourfold shell filling of holes. (**D**) (Inset) The mechanical resonance induces a corresponding resonance in the dc current which can have a narrow linewidth with Q up to 150,000. (Main plot) The resonance frequency can be tuned using a tensioning force from the dc voltage on the gate.

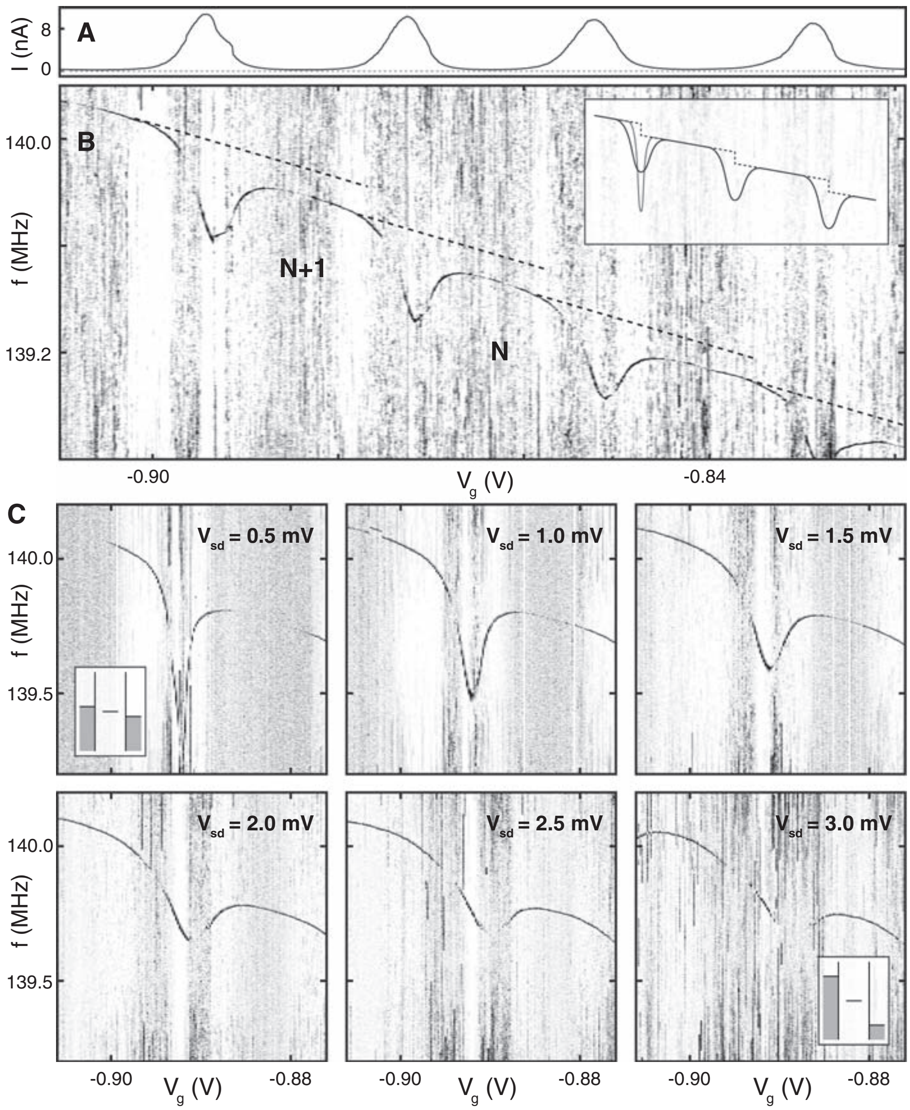

Fig. 2. Single-electron tuning. (**A**) Nanotube current versus gate voltage showing single-electron tunneling at the peaks and Coulomb blockade in the valleys. This curve is taken from (B) at $f = 138.8$ MHz. (**B**) Normalized resonance signal $\Delta I/\Delta I_{peak}$ (see SOM) versus RF frequency and gate voltage ($V_{sd} = 1.5$ mV). The tuned mechanical resonance shows up as the darker curve with dips at the Coulomb peaks. The offsets between the dashed lines indicate the frequency shift due to the addition of one electron to the nanotube. The resonance frequency also shows dips caused by a softening of the spring constant because of single-electron charge fluctuations. N, number of holes on the quantum dot. (Inset) The expected resonance behavior (see text). (**C**) Zoom-in view on one frequency dip for various source-drain voltages (V_{sd}) showing dip broadening for increasing V_{sd}. (Insets) Energy diagrams for small and large V_{sd}.

We actuate the resonator with a nearby antenna and detect the resonator motion by its influence on the dc current through the nanotube. The inset to Fig. 1D shows a peak in the current at the resonance frequency, which we have identified as a bending-mode mechanical resonance of the nanotube (*12*). Q typically exceeds 10^5, which is an increase of more than two orders of magnitude compared with previous nanotube studies (*4*, *17*, *18*). The resonance frequency is tuned by more than a factor of 2 with the gate voltage (Fig. 1D). The electric field from the gate pulls the nanotube toward it, and the subsequent lengthening of the nanotube induces more tension, similar to the tuning of a guitar string (*17*).

Our detection signal results from a change in the gate capacitance (ΔC_g) during a displacement of the nanotube. This changes the effective quantum-dot potential and, if positioned initially beside a Coulomb peak (Fig. 1C), can move it onto the peak, thereby increasing the current. For a nanotube oscillating on resonance, the effective potential oscillates, and the nonlinearity of Coulomb blockade allows it to be rectified to a detectable dc current.

The narrow linewidth of the resonance peak provides an unprecedented sensitive probe for studying nanomechanical motion. We first show the influence of a single electron on the resonance frequency (f_0). The Coulomb oscillations in Fig. 2A are caused by single-electron tunneling giving rise to current peaks, and Coulomb blockade fixes the electron number in the valleys. From valley to valley, the electron number changes by one. Figure 2B shows the mechanical resonance signal recorded at the same time. Overall, a more negative gate voltage (right to left) increases the total charge on the nanotube, increasing the tension. This process stiffens the mechanical spring constant and increases the resonance frequency. Linear stiffening occurs in the Coulomb valleys (indicated with dashed lines), whereas at Coulomb peaks, a peculiar softening occurs, which is visible as dips in f_0.

We first focus on the change in resonance frequency caused by the addition of one electron, which is measured as offsets of ~0.1 MHz between the dashed lines. This shift from single-electron tuning, predicted in (*19*), is ~20 times our linewidth and thus clearly resolvable. Because we compare valleys with a fixed electron number, this single-electron tuning comes from a change in a static force on the nanotube. The (electro-) static force is proportional to the square of the charge on the nanotube and, thus, adding one electron charge results here in a detectable shift in the mechanical resonance (*19*). The shifts from single-electron tuning can be as large as 0.5 MHz, more than 100 times the line width (*20*).

Next we focus on the dips in resonance frequency that occur at the Coulomb peaks. The current at the Coulomb peaks is carried by single-electron tunneling, meaning that one electron tunnels off the nanotube before the next electron can enter the tube. The charge on the nanotube fluctuates by exactly one electron charge (e) with a time dynamics that can be accounted for in detail by the theory of Coulomb blockade (*21*). The average rate (Γ) at which an electron moves across the tube can be read off from the current $I = e\Gamma$ (1.6 pA corresponds to a 10-MHz rate). Moving the gate voltage off or on a Coulomb peak, we can tune the rate from the regime $\Gamma \sim f_0$ to $\Gamma >> f_0$ and explore the different effects on the mechanical resonance.

In Fig. 2, A and B, the Coulomb peak values of ~8 nA yield $\Gamma \sim 300 f_0$, the regime of many single-electron tunneling events per mechanical oscillation. In addition to the static force and the radio frequency (RF) oscillating driving force, single-electron tunneling now exerts a time-fluctuating, dynamic force on the mechanical resonator. We observe that this dynamic force causes softening, giving dips in the resonance frequency. The single-electron charge fluctua-

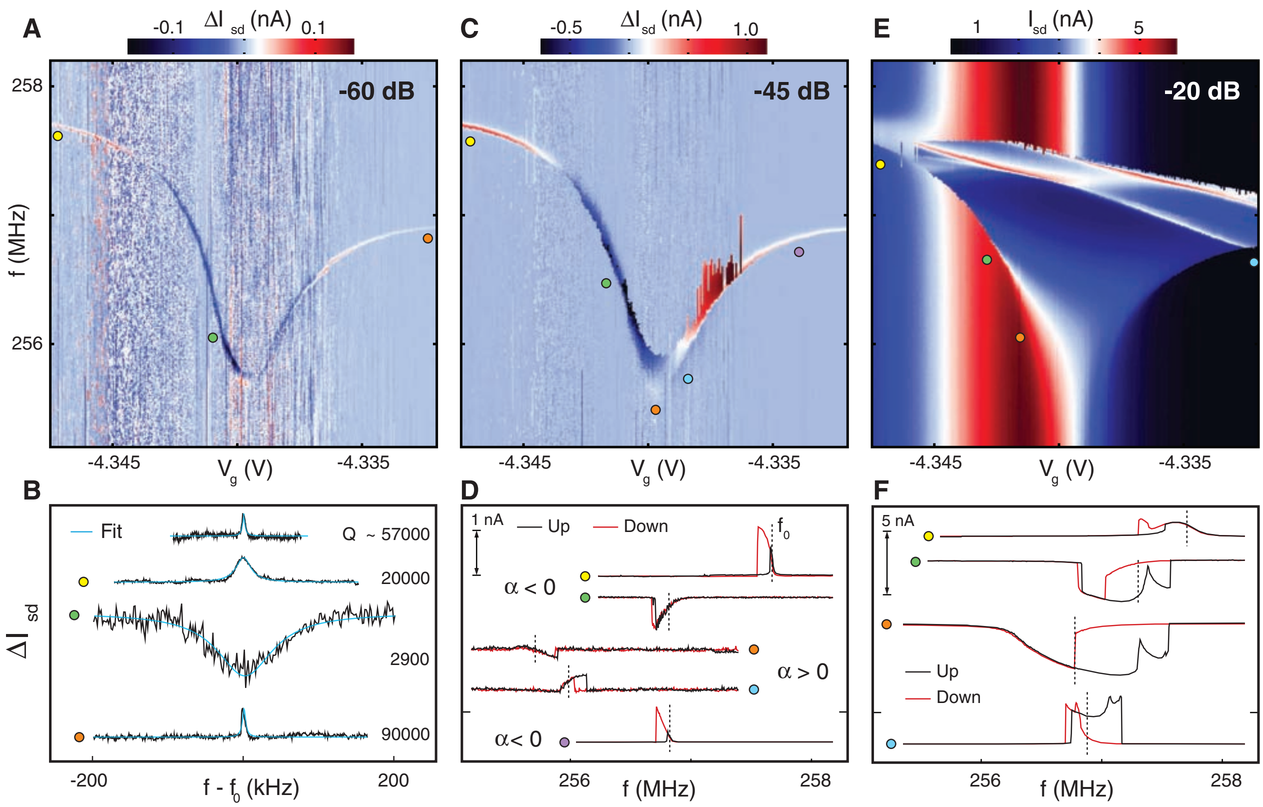

Fig. 3. Line shapes of the mechanical resonance from linear to nonlinear driving regimes. (**A**) Detector current(ΔI) versus frequency and gate-voltage at RF excitation power of –60 dB, as the gate voltage is swept through one Coulomb peak. (**B**) Fits of the resonance to a squared Lorentzian line shape at different gate voltages (*12*). The RF power for each trace is adjusted to stay in the linear driving regime (–75, –64, –52, and –77 dB, top to bottom). Traces are taken at the positions indicated by colored circles (aside from the top trace, which is taken at V_g = –4.35 V). (**C**) At –45 dB, the resonance has an asymmetric line shape with one sharp edge; see linecuts (**D**), typical for a nonlinear oscillator (*23*, *24*). Dashed lines in (D) and (F) indicate resonance frequency f_0 at low powers. (**E and F**) At even higher driving powers (–20 dB), the mechanical resonator displays sharp subpeaks and several jumps in amplitude when switching between different stable modes. (C) and (E) are taken in the upward sweep direction (downward sweeps shown in the SOM).

tions do not simply smooth the stepwise transition from the static single-electron tuning shifts. Instead, fluctuations caused dips in the resonant frequency up to one order of magnitude greater than the single-electron tuning shifts. As shown in (*13*, *22*) and discussed in detail in the supporting online material (SOM) (*20*), the dynamic force modifies the nanotube's spring constant (k) resulting in a softening of the mechanical resonance. The shape of the frequency dip can be altered by applying a finite bias (V_{sd}) across the nanotube. Starting from deep and narrow at small V_{sd} = 0.5 mV, the dip becomes shallower and broader with increasing V_{sd}. This dip shape largely resembles the broadening of Coulomb blockade peaks that occurs with increasing V_{sd}. Thus, we conclude from Fig. 2 that the single-electron tuning oscillations are a mechanical effect that is a direct consequence of single-electron tunneling oscillations.

Besides softening, the charge fluctuations also provide a channel for dissipation of mechanical energy. Figure 3A shows the resonance dip for small RF power, with frequency traces in Fig. 3B. In the Coulomb valleys, tunneling is suppressed ($\Gamma \sim f_0$), damping of the mechanical motion is minimized, and we observe the highest value of Q. On a Coulomb peak, charge fluctuations are maximized ($\Gamma >> f_0$), and Q decreases to a few thousand. These results explicitly show that detector back-action can cause substantial mechanical damping. The underlying mechanism for the damping is an energy transfer occasionally occurring when a current-carrying electron is pushed up to a higher (electrostatic) energy by the nanotube motion before tunneling out of the dot. This gain in potential energy is later dissipated in the drain contact.

If we drive the system at higher RF powers (Fig. 3, C and D), we observe an asymmetric resonance peak, along with distinct hysteresis between upward and downward frequency sweeps. Theoretically, this marks the onset of nonlinear terms in the equation of motion, such as in the well-studied Duffing oscillator (*23*, *24*). k is modified by a large oscillation amplitude (x) that is accounted for by replacing k with ($k + \alpha x^2$). The time-averaged spring constant increases if $\alpha > 0$, which is accompanied by a sharp edge at the high-frequency side of the peak; vice versa for $\alpha < 0$. In addition to the overall softening of k yielding the frequency dips of Fig. 2, the fluctuating charge on the dot also changes α, giving a softening spring ($\alpha < 0$) outside of the frequency dip (Coulomb valleys) and a hardening spring ($\alpha > 0$) inside the frequency dip (Coulomb peaks), as shown in Fig. 3. The sign of α follows the curvature of $f_0(V_g)$ induced by the fluctuating electron force, giving a change in sign at the inflection point of the frequency dip. Nonlinearity from the single-electron force in our device dominates and is much stronger than that from the mechanical deformation (*20*).

Figure 3, E and F, shows the regime of further enhanced RF driving. Now the nonlinearity is no longer a perturbation of the spring constant, but instead gives sharp peaks in the line shape and switching between several different metastable modes [see further data in the SOM (*20*)]. At this strong driving, we observe highly structured nonlinear mechanical behavior that arises from the coupling of the resonator motion to the quantum dot.

In Fig. 3, we studied nonlinear coupling between the quantum dot and the mechanical resonator by applying a large RF driving force at a

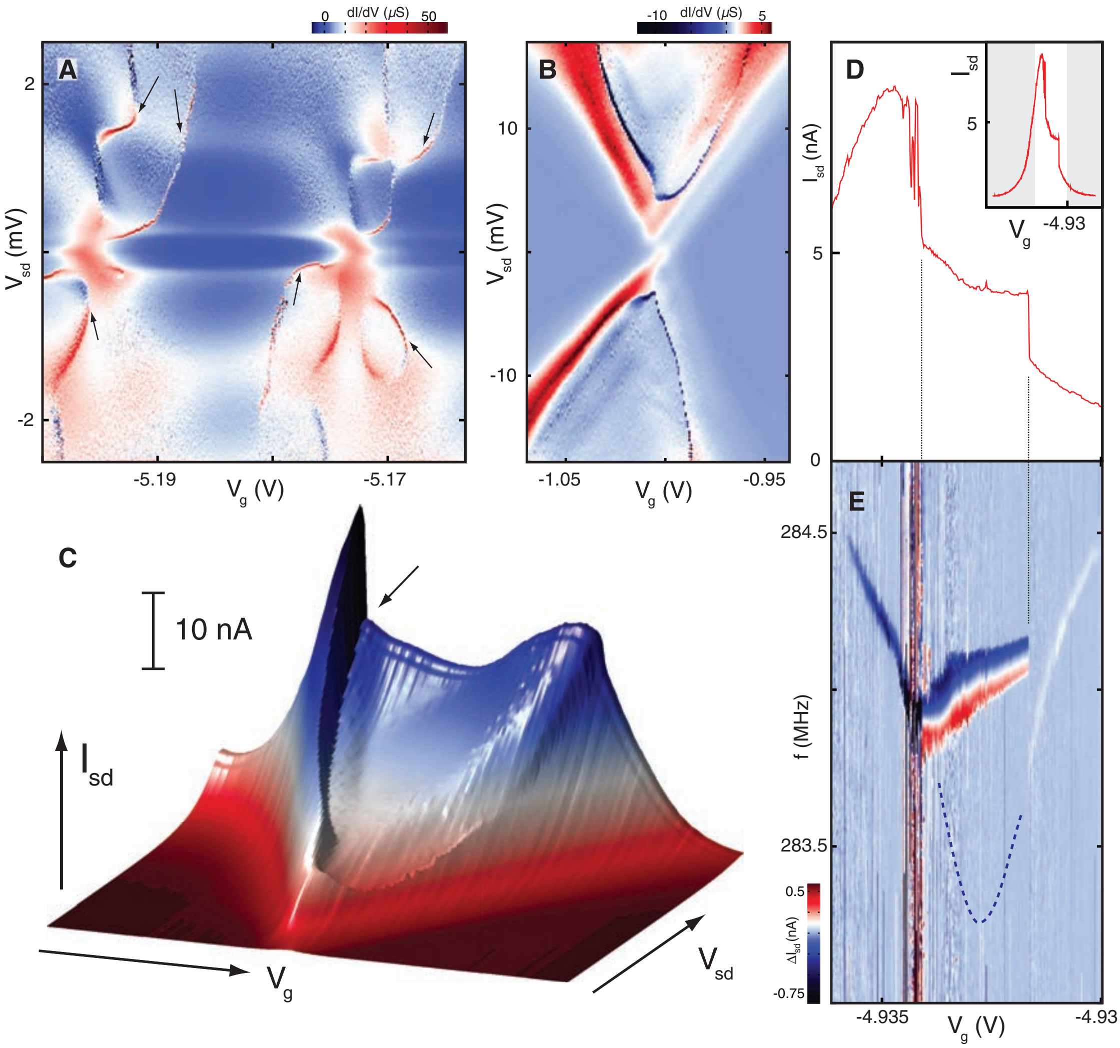

Fig. 4. Spontaneous driving of the mechanical resonance by single-electron tunneling. (**A**) Differential conductance (dI/dV_{sd}) showing ridges of sharp positive (deep red) and negative (deep blue) spikes (arrows). (**B**) Similar ridges measured on device two (trench width = 430 nm) in the few-hole regime (four-hole–to–three-hole transition). Spikes in dI/dV_{sd} appear as steplike ridges in current. (**C**) shows the data from the upper half of (B), but now as a three-dimensional current plot. The ridges are entirely reproducible. (**D**) (Inset) Coulomb peak at V_{sd} = 0.5 mV showing large switching-steps. (Main plot) Zoom-in view on data from inset. (**E**) RF driven mechanical resonance measured for the same Coulomb peak in (D) at a driving power of –50 dB. Outside the switch region, the resonance has a narrow line shape and follows the softening dip from Figs. 2 and 3. At the first switch, the resonance position departs from the expected position (indicated by dashed line). The mechanical signal is strongly enhanced in amplitude and displays a broad asymmetric line shape. At the second switch, the resonance returns to the frequency and narrow line shape expected at these powers.

small V_{sd}. In Fig. 4, we consider small or absent RF driving force and now apply a large V_{sd} across the quantum dot. Figure 4A shows a standard Coulomb blockade measurement of the quantum dot. Mechanical effects in Coulomb diamonds have been studied before in the form of phonon sidebands of electronic transitions (*25*–*28*). Shown in the data of Fig. 4 are reproducible ridges of positive and negative spikes in the differential conductance as indicated by arrows. This instability has been seen in all 12 measured devices with clean suspended nanotubes and never in nonsuspended devices. Figure 4, B and C, shows such ridges in a second device, visible as both spikes in the differential conductance (Fig. 4B) and discrete jumps in the current (Fig. 4C). The barriers in device two were highly tunable: We found that the switch-ridge could be suppressed by reducing the tunnel coupling to the source-drain leads, thereby decreasing the current. The instability disappears roughly when the tunnel rate is decreased below the mechanical resonance frequency (see SOM) (*20*).

In a model predicting such instabilities (*29*), positive feedback from single-electron tunneling excites the mechanical resonator into a large-amplitude oscillation. The theory predicts a characteristic shape of the switch-ridges and the suppression of the ridges for $\Gamma \sim f_0$, in marked agreement with our observations. Such feedback also requires a very high Q, which may explain why it has not been observed in previous suspended quantum-dot devices (*26*, *28*). If the required positive feedback is present, however, it should also have a mechanical signature; such a signature is demonstrated in Fig. 4E. The RF-driven mechanical resonance experiences a dramatic perturbation triggered by the switch-ridge discontinuities in the Coulomb peak current shown in Fig. 4D. At the position of the switch, the resonance peak shows a sudden departure from the expected frequency dip (dashed line) and becomes strongly asymmetric and broad, as if driven by a much higher RF power. This is indeed the case, but the driving power is now provided by an internal source: Because of the strong feedback, the random fluctuating force from single-electron tunneling becomes a driving force coherent with the mechanical oscillation. Remarkably, the dc current through the quantum dot can be used both to detect the high-frequency resonance and, in the case of strong feedback, directly excite resonant mechanical motion.

References and Notes

1. H. G. Craighead, *Science* **290**, 1532 (2000).
2. K. L. Ekinci, M. L. Roukes, *Rev. Sci. Instrum.* **76**, 061101 (2005).
3. K. L. Ekinci, X. M. H. Huang, M. L. Roukes, *Appl. Phys. Lett.* **84**, 4469 (2004).
4. B. Lassagne, D. Garcia-Sanchez, A. Aguasca, A. Bachtold, *Nano Lett.* **8**, 3735 (2008).
5. H.-Y. Chiu, P. Hung, H. W. Postma, M. Bockrath, *Nano Lett.* **8**, 4342 (2008).
6. R. G. Knobel, A. N. Cleland, *Nature* **424**, 291 (2003).
7. M. D. LaHaye, O. Buu, B. Camarota, K. C. Schwab, *Science* **304**, 74 (2004).
8. A. Naik *et al.*, *Nature* **443**, 193 (2006).
9. K. C. Schwab, M. L. Roukes, *Phys. Today* **58**, 36 (2005).
10. C. M. Caves, K. S. Thorne, R. W. Drever, V. D. Sandberg, M. Zimmermann, *Rev. Mod. Phys.* **52**, 341 (1980).
11. C. A. Regal, J. D. Teufel, K. W. Lehnert, *Nat. Phys.* **4**, 555 (2008).
12. A. K. Hüttel *et al.*, *Nano Lett.* **9**, 2547 (2009).
13. M. T. Woodside, P. L. McEuen, *Science* **296**, 1098 (2002).
14. J. Zhu, M. Brink, P. L. McEuen, *Appl. Phys. Lett.* **87**, 242102 (2005).
15. R. Stomp *et al.*, *Phys. Rev. Lett.* **94**, 056802 (2005).
16. G. A. Steele, G. Gotz, L. P. Kouwenhoven, *Nat. Nano.* **4**, 363 (2009).
17. V. Sazonova *et al.*, *Nature* **431**, 284 (2004).
18. B. Witkamp, M. Poot, H. S. J. van der Zant, *Nano Lett.* **6**, 2904 (2006).
19. S. Sapmaz, Y. Blanter, L. Gurevich, H. S. J. van der Zant, *Phys. Rev. B* **67**, 235414 (2003).
20. Supporting online material is available on *Science* Online.
21. C. W. J. Beenakker, *Phys. Rev. B* **44**, 1646 (1991).
22. M. Brink, thesis, Cornell Univerity (2007).
23. A. Cleland, *Foundations of Nanomechanics* (Springer, Berlin, 2002).
24. A. H. Nayfeh, D. T. Mook, *Nonlinear Oscillations* (Wiley, New York, 1979).
25. H. Park *et al.*, *Nature* **407**, 57 (2000).
26. S. Sapmaz, J. P. Herrero, Ya. M. Blanter, C. Dekker, H. S. J. van der Zant, *Phys. Rev. Lett.* **96**, 026801 (2006).
27. F. A. Zwanenburg, C. E. van Rijmenam, Y. Fang, C. M. Lieber, L. P. Kouwenhoven, *Nano Lett.* **9**, 1071 (2009).
28. R. Leturcq *et al.*, *Nat. Phys.* **5**, 327 (2009).
29. O. Usmani, Y. M. Blanter, Y. V. Nazarov, *Phys. Rev. B* **75**, 195312 (2007).

30. We thank Y. M. Blanter and Y. V. Nazarov for helpful discussions. This work was supported by the Dutch Organization for Fundamental Research on Matter, the Netherlands Organization for Scientific Research, the Nanotechnology Network Netherlands, and the Japan Science and Technology Agency International Cooperative Research Project.

Supporting Online Material
www.sciencemag.org/cgi/content/full/1176076/DC1
Materials and Methods
SOM Text
Figs. S1 to S6
References

11 May 2009; accepted 13 July 2009
Published online 23 July 2009;
10.1126/science.1176076
Include this information when citing this paper.

Coupling Mechanics to Charge Transport in Carbon Nanotube Mechanical Resonators

Benjamin Lassagne,[1]* Yury Tarakanov,[2] Jari Kinaret,[2] David Garcia-Sanchez,[1] Adrian Bachtold[1]†

Nanoelectromechanical resonators have potential applications in sensing, cooling, and mechanical signal processing. An important parameter in these systems is the strength of coupling the resonator motion to charge transport through the device. We investigated the mechanical oscillations of a suspended single-walled carbon nanotube that also acts as a single-electron transistor. The coupling of the mechanical and the charge degrees of freedom is strikingly strong as well as widely tunable (the associated damping rate is ~3×10^6 Hz). In particular, the coupling is strong enough to drive the oscillations in the nonlinear regime.

Carbon nanotubes have been used to fabricate mechanical resonators that can be operated at ultrahigh frequencies, have widely tunable resonance frequencies, and can be used as ultrasensitive inertial mass sensors (*1*–*10*). In addition, carbon nanotubes also have exceptional electron transport properties, including ballistic conduction over long distances or multiple Coulomb blockade–related phenomena that can be observed even up to room temperature (*11*). Coupling the mechanical motion of nanotube resonators to electron transport is thus highly appealing. In particular, we would like to use such a coupling as a way to control the mechanical motion at the nanoscale. Recently, microfabricated silicon resonators have been fabricated whose mechanical vibrations are damped by cooling from a nearby superconducting single-electron transistor (*12*). In the case of nanotube resonators, however, the extent to which it is possible to couple mechanical vibrations and charge transport is not clear.

We studied the coupling between the mechanics and the electron transport of a single-walled carbon nanotube (SWNT) resonator at cryogenic temperature in which conducting electrons enter the Coulomb-blockade regime. We show that single electrons tunneling into and out of the nanotube greatly affect the nanotube motion. The coupling can be made stronger than in nanoelectromechanical systems (NEMS) resonators studied so far, including those fabricated in silicon by using top-down approaches. Moreover,

[1]Centre d'Investigació en Nanociència i Nanotecnologia (Consejo Superior de Investigaciones Científicas–Institut Català de Nanotecnologia), campus Universitat Autònoma de Barcelona, E-08193 Barcelona, Spain. [2]Department of Applied Physics, Chalmers University of Technology, SE-41296 Göteborg, Sweden.

*Present address: Université de Toulouse, Université Paul Sabatier, Institut National des Sciences Appliquées, UMR 5215 Laboratoire de Physique et Chimie de Nano-Objets CNRS, F-31077 Toulouse, France.

†To whom correspondence should be addressed. E-mail: adrian.bachtold@cin2.es